# Conductivity and permeability of rocks

Po-zen Wong, Joel Koplik, and J. P. Tomanic
*Schlumberger-Doll Research, Old Quarry Road, Ridgefield, Connecticut 06877-4108*
(Received 20 July 1984)

The electrical conductivity of salt-water-saturated rocks is modeled by a random resistance network which has a zero percolation threshold. The porosity is varied by a random bond-shrinkage mechanism. Numerical and analytical calculations of the model in different dimensions show an Archie's-law behavior: $\sigma_r = a\sigma_w \phi^m$, where $\phi$ is the porosity of the rock, and $\sigma_r$ and $\sigma_w$ are the conductivities of the rock and water, respectively. We find that the Archie's exponent $m$ is always greater than unity and is related to the skewness of the "pore-size distribution" of the rock. Applying the same model to fluid-flow permeability ($k_r$) gives $k_r \propto \phi^{m'}$, where $m' = m(m+1)$ in one dimension, and $m' = 2m$ in higher dimensions. This power-law form is consistent with the well-known Kozeny equation and has been frequently suggested by empirical studies. Experimental tests of the model are performed on artificial rocks, made by fusing small glass beads, as well as real rocks. From resistivity measurements, we demonstrate that $m$ is larger in samples with a wider fluctuation of pore sizes, which is qualitatively consistent with the model. From fluid-flow experiments on fused glass beads, we find quantitative support for the $m' = 2m$ prediction.

## I. INTRODUCTION

An interesting geometrical feature of rocks is that they appear not to have a finite percolation threshold. When their pore space is saturated with salt water, they exhibit finite electrical conductivity ($\sigma_r$) even when the porosity ($\phi$) is below 1%. An empirical equation that links the conductivity and the porosity was first proposed by Archie and has become known as Archie's law:[1]

$$\sigma_r = a\sigma_w \phi^m , \tag{1}$$

where $\sigma_w$ is the conductivity of the water, and $a$ and $m$ are empirical parameters that vary with the lithology of the rock formation. Quite often, $a$ is assumed to be unity and $m \approx 2$. The power-law dependence in this equation resembles the behavior in the usual percolation problem, except that it suggests a conduction threshold at $\phi = 0$. In addition, the exponent $m$ is not entirely universal; different values have been given by Keller for different kinds of formation.[2]

For fluid flow through a rock, another empirical law, known as the Kozeny equation, relates the permeability ($k_r$) to the porosity:[3]

$$k_r = c\frac{\phi^3}{S_0^2} , \tag{2}$$

where $S_0$ is the specific surface area (i.e., internal surface area per unit bulk volume) of the rock and $c$ ($\approx 0.2$) is an empirical constant. This equation again has both a power-law dependence on the porosity and the suggestion that the pore space is connected at any finite porosity.

Historically, these empirical relationships were justified by modeling the pore space as a bundle of winding tubes which do not intersect each other. With that assumption, both equations above can be easily derived.[4-6] Such a model is highly unrealistic, however, since any micrograph of a thin section of a rock would show that the pore space is multiply connected in a complicated and random way. In Fig. 1 we show micrographs for two sandstones and one limestone as illustrations. It should be clear from these pictures that a more appropriate model of the pore space should involve some kind of random network. Indeed, such an approach has been widely used in the last three decades to simulate the petrophysical properties of rock formations and to study the behavior of other porous media. A glance at the literature, however, indicates that a basic understanding has not emerged from these studies. We shall refer the readers to Refs. 5 and 6 for a survey of these studies and not attempt to discuss them here.

In more recent years, Sen, Scala, and Cohen[7] have proposed a self-similar model to explain Archie's law, by considering the geometry of the grain space to be a random assemblage of spheres of all radii. In essence, they applied Bruggeman's theory[8] which integrated the classical Clausius-Mossotti equation for noninteracting dielectric spheres embedded in a homogeneous media from the $\phi = 1$ dilute limit (hence, the model is also known as the "iterated dilute limit"), and this gives $m = \frac{3}{2}$. This method is attractive in that it intrinsically preserves the pore-space connectivity for any value of $\phi$. Furthermore, other values of $m$ can be obtained if spheroids with different aspect ratios are used.[7-9] Experimental support for the iterated dilute result can be found in the work of De La Rue and Tobias.[10] They measured the conductivity of dilute suspensions of glass spheres, polystyrene cylinders, and sand grains in $ZnBr_2$ solutions for $\phi \geq 0.60$ and found $m \approx 1.5$ in each case.

Using the self-similar model to understand the behavior of rocks presents two difficulties. First, one knows that rocks generally have porosities less than 40%, which is far from the dilute limit in which the assumptions of the model have the most justification. When the porosity is low, the grains are in close contact and the interactions

 

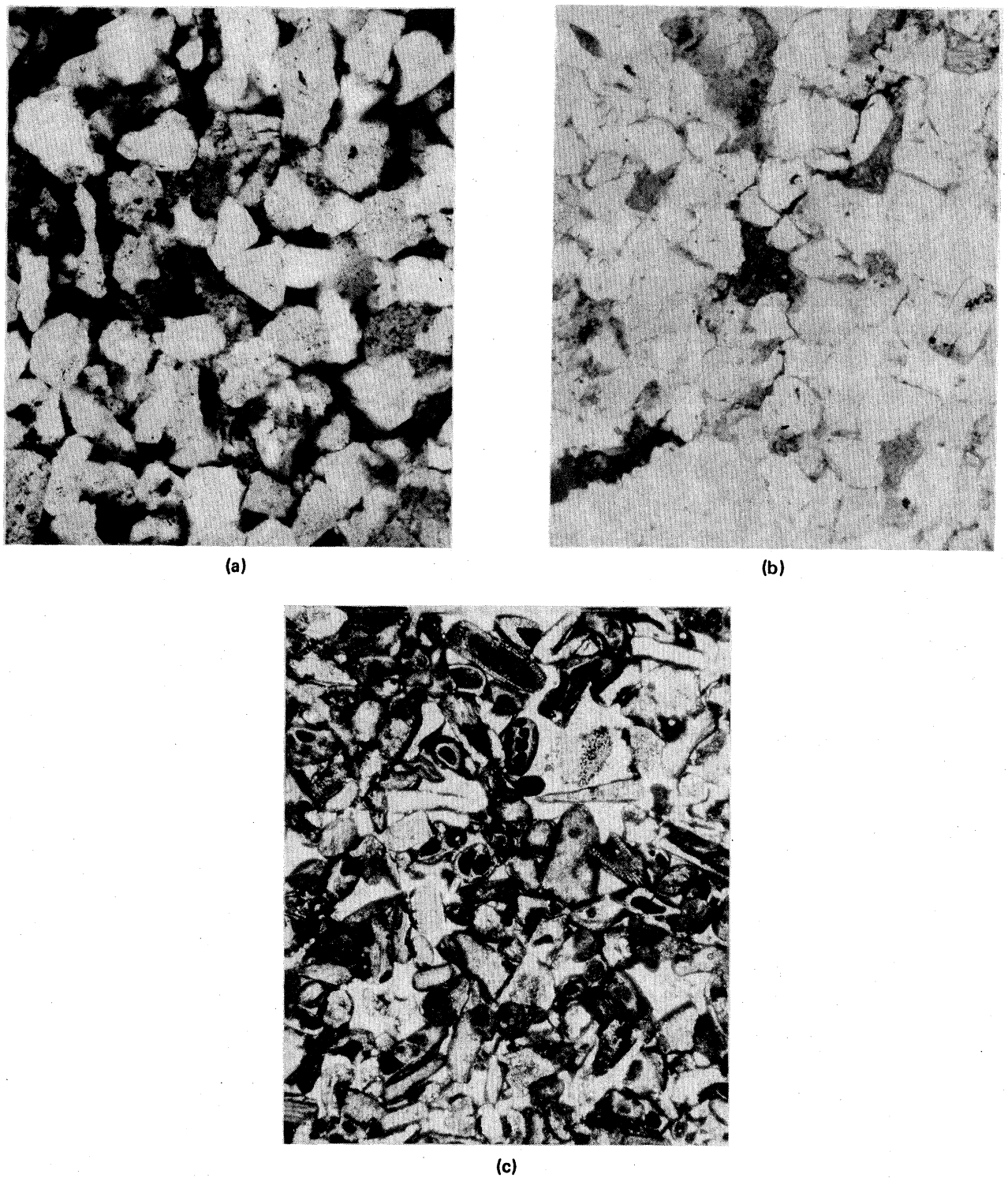


FIG. 1. Thin section micrographs of (a) Berea sandstone (100×), (b) Cotton Valley sandstone (100×) and (c) Indiana limestone (25×). The pore space in (a) and (b) are dark whereas, in (c), it is bright. The grain shapes of (a) and (b) are very similar, but they have different $m$'s. The grain shapes of (b) and (c) are very different, but their $m$ values are essentially the same.

between them are important. Recently, Milton[11] has shown that the self-similar model accounts for the interactions correctly only in a special hierarchical geometry in which grains of any particular size are surrounded by much smaller grains and grains of the same size are far separated from each other. A glance at Fig. 1 shows that real rocks do not possess such a geometry. Instead, they usually have a characteristic grain size (of order 100 $\mu$m) and these grains are in contact with each other. Second, from an experimental point of view, we find that in rocks

with similar grain shapes the exponent $m$ can vary significantly and, conversely, in rocks with very different grain shapes the values of $m$ can be very similar. For example, resistivity measurements on the three samples shown in Fig. 1 give $m=1.94$ for the Cotton Valley sandstone and $m=1.65$ for the Berea sandstone [assuming $a=1$ in Eq. (1)], but these two rocks have similar grain shapes. For the Indiana limestone, which has visibly different grain shapes from the two sandstones, we find $m=1.95$, essentially the same as that for the Cotton Valley sandstone. These comparisons cannot be explained by a grain-shape effect.

In this paper, *we focus our attention on the variation of the pore space with porosity and show how the "pore-size distribution" can influence the conductivity and permeability.* In Sec. II we introduce a tractable random network model which exploits the similarity to the bond-percolation problem. We consider a lattice of random-sized cylinders, and systematically reduce the volume of pore space by randomly shrinking their radii. Although the model is not completely realistic, we will show how it allows us to qualitatively understand the meaning of Archie's law and the Kozeny equation. Through this improved understanding, we can suggest a modified form for the Kozeny equation which relates the permeability to the conductivity. In Sec. III we describe the results of some simple conductivity and permeability experiments performed on artificial rocks (Ridgefield sandstones) made of fused glass spheres, which provide good support for the theoretical predictions. Some further discussion will be given in Sec. IV, where we clarify what we mean by "pore-size distribution" and argue that *the unrealistic elements in our model do not affect the main conclusions that we draw from it.*

## II. BOND-SHRINKAGE MODEL

Our model is motivated by the similarity of Eqs. (1) and (2) to the scaling laws that are characteristic of the percolation problem, keeping in mind that we want to make the conduction threshold occur at $\phi=0$. We consider a random resistor network on a simple cubic lattice in $d$ dimensions. Each resistor $R_i$ represents a cylindrical fluid-filled tube with radius $r_i$. In the usual bond-percolation problem, one chooses a conductance element at random and sets its radius equal to zero. This procedure results in a finite conduction threshold $p_c(d)$, for when the concentration of unbroken bonds $p$ is less than $p_c$, the network becomes disconnected and ceases to conduct. The formation of a sedimentary rock, however, is a somewhat different process. There, one imagines, that the rock begins as a packing of unconsolidated grains, which is analogous to a fully connected network, with some initial conductivity and porosity ($\sim 40\%$). In the course of time, the cross section of any conduction channel can be reduced by the pressure on the rock, by further deposition of smaller particles, or by other mechanisms. The porosity and the conductivity will, as result, be reduced simultaneously. The probability of the channel becoming completely blocked is, however, very small. For example, consolidation of the wall of the channel under pressure reduces the local stress, strengthens the wall, and resists further deformation. Deposition of irregularly shaped particles in an irregularly shaped channel can never completely block that channel, regardless of how many such particles are deposited. Furthermore, thin lubricating films of fluid, if present, will inhibit grain contact. To model such behavior in our network, we randomly choose a tube element and reduce its radius by a fixed factor $x$,

$$r_i \rightarrow x r_i \ , \tag{3}$$

where $0<x<1$ and $i$ is randomly chosen. Since the electrical conductance of a given tube is proportional to its cross-sectional area, it will decrease by a factor $x^2$. Similarly, the permeability of a cylinder (the ratio of fluid flux to pressure difference) is proportional to $r_i^4$ and would be reduced by a factor $x^4$. This shrinking procedure can be repeated indefinitely with the same $x$ to reduce the network conductance and permeability, and the total volume of the tubes. The length of the tube is kept unchanged, so that if channel $i$ is chosen $n$ times, its conductance will be reduced from $G_i$ to $x^{2n}G_i$, and its permeability from $k_i$ to $x^{4n}k_i$. We will neglect the nodes at which the tubes are connected. Although this is unrealistic, we will argue in Sec. IV that *this and other artificial elements in the model, such as assigning uniform radii to the tubes, shrinking them by a constant factor, etc., do not affect the conclusions that we will derive from the model.* It is only important to note at this point that the model has two attractive features: (i) it preserves the network connectivity in the $\phi \rightarrow 0$ limit for any $x>0$ and (ii) the amount of change in $r_i$ at any shrinking step is dependent on the value of $r_i$ at that time. Both of these features are crucial in obtaining the behavior of Eqs. (1) and (2). If we consider the limiting case $x=0$, this model coincides with the usual bond-percolation problem and there will be a finite percolation threshold.

### A. Solution in one dimension

To see that this model leads to Archie's law and the Kozeny equation, we first solve it exactly (and trivially) in one dimension (1D). We consider $N$ tubes connected in series and shrink them randomly according to Eq. (3) a total of $M$ times. Since we keep the tube length $l$ constant, the total volume (or porosity) of this 1D network is proportional to the *average* cross section, and hence the *average* conductance $\langle G \rangle$. To calculate $\phi$, we note that the probability for any particular tube to shrink $n$ times is simply given by the binomial distribution

$$P(n)=\frac{M!}{(M-n)!n!}\left[\frac{1}{N}\right]^n\left[\frac{N-1}{N}\right]^{M-n} . \tag{4}$$

The *average* conductance of that tube is

$$\bar{G}_i=G_i\sum_{n=0}^{M}x^{2n}P(n)=G_i\left[\frac{N+x^2-1}{N}\right]^M . \tag{5}$$

The *average* conductance of the whole 1D network is therefore

$$\langle G\rangle=\langle\bar{G}_i\rangle=\langle G_i\rangle\left[\frac{N+x^2-1}{N}\right]^M, \tag{6}$$

where $\langle\ \rangle$ denotes the averaging over the network, which is decoupled from the average over the shrinkage probability $P(n)$ for an individual tube in Eq. (5). The *true* conductance of the network $G_{\rm nw}$ is not $\langle G\rangle$. Instead, since the resistors are in series,

$$\begin{aligned}G_{\rm nw}^{-1}=R_{\rm nw}&=N\langle\bar{R}_i\rangle=N\langle\overline{G_i^{-1}}\rangle\\&=N\langle G_i^{-1}\rangle\sum_{n=0}^{M}x^{-2n}P(n)\\&=N\langle G_i^{-1}\rangle\left[\frac{N+x^{-2}-1}{N}\right]^M.\end{aligned} \tag{7}$$

When the number of tubes is large, we have

$$\begin{aligned}\lim_{N\to\infty}\frac{\ln(R_{\rm nw}/N\langle G_i^{-1}\rangle)}{\ln(\langle G\rangle/\langle G_i\rangle)}&=\lim_{N\to\infty}\frac{\ln[1+(x^{-2}-1)/N]}{\ln[1+(x^2-1)/N]}\\&=\frac{x^{-2}-1}{x^2-1}=-\frac{1}{x^2},\end{aligned} \tag{8}$$

which implies

$$R_{\rm nw}\propto\langle G\rangle^{-1/x^2} \tag{9}$$

for an infinite system. Since $\phi\propto\langle G\rangle$, we have Archie's law,

$$G_{\rm nw}\propto\phi^m \quad\text{where } m=\frac{1}{x^2}>1. \tag{10}$$

When $x\to0$, we have $m\to\infty$ and hence $G_{\rm nw}\to0$ for any $\phi<1$, which is the correct behavior for 1D percolation. *The dependence of m on x indicates that the network conductance is sensitive to the distribution of the tube radii. The reason that $m>1$ is that the network conductance $G_{\rm nw}$ and the porosity $\phi$ depend on the distribution in different ways: $G_{\rm nw}$ is influenced mainly by the narrow tubes and $\phi$ is influenced mainly by the wide tubes.* Our model allows us to obtain an exact solution to demonstrate this simple fact explicitly.

The above calculation can be easily modified to give the fluid-flow permeability of the network. Since the permeability of a single tube element is $k_i\propto r_i^4$, to calculate the network permeability in 1D, we simply replace $x^{-2}$ in Eq. (7) by $x^{-4}$. Repeating the steps in Eqs. (8)—(10), we obtain

$$k_{\rm nw}\propto\phi^{m'} \quad\text{where } m'=m(m+1)>2m, \tag{11}$$

which is analogous to the Kozeny equation [Eq. (2)] except for the factor $1/S_0^2$. This factor may be inserted on the basis of dimension analysis because permeability has the dimension of [length]$^2$ and $1/S_0\equiv$(volume/area) is a natural unit of length in a porous material. On the other hand, many studies have suggested the use of other characteristic lengths, such as the average particle size.[6] More will be said about this in Sec. IV. The fact that $m'>m$ shows that the permeability is more strongly dependent on the tube-size fluctuation than the conductivity. More importantly, it shows that both quantities are governed by the tube-size distribution and they can be simply related, at least in one dimension.

### B. Numerical results in higher dimensions

If we consider the same bond-shrinkage model in higher dimensions ($d\geq2$), we note that while the porosity is still given by Eq. (6), the network conductance is not given by Eq. (7). To calculate $G_{\rm nw}$, one can apply the Kirchoff's law to finite-size samples and solve the network equations numerically. We use this approach on simple cubic networks of dimension $L^{d-1}(L+1)$. The boundary conditions are (i) constant potential at the two ends of the long dimension, and (ii) periodic in the $d-1$ transverse directions. Typically, we assign an initial set of $r_i$'s to each bond, which has a flat distribution in the range $0<r_i<1$. The initial porosity $\phi(\equiv\langle r_i^2\rangle)$ is defined to be unity. We also let $G_i=r_i^2$ and $k_i=r_i^4$, i.e., all the prefactors are defined to be unity. The $r_i$'s are then randomly reduced by the fixed factor $x$ as in Eq. (3). When $\phi$ is reduced by a factor of 2, we calculate the network conductance $G_{\rm nw}$ and permeability $k_{\rm nw}$. The process is repeated until $\phi$ is reduced by about three orders of magnitude. For any set of values for the sample parameters $d$, $L$, and $x$, we repeated the calculation for ten initial sets of $r_i$'s and average the results to improve the statistics. Figure 2 shows a

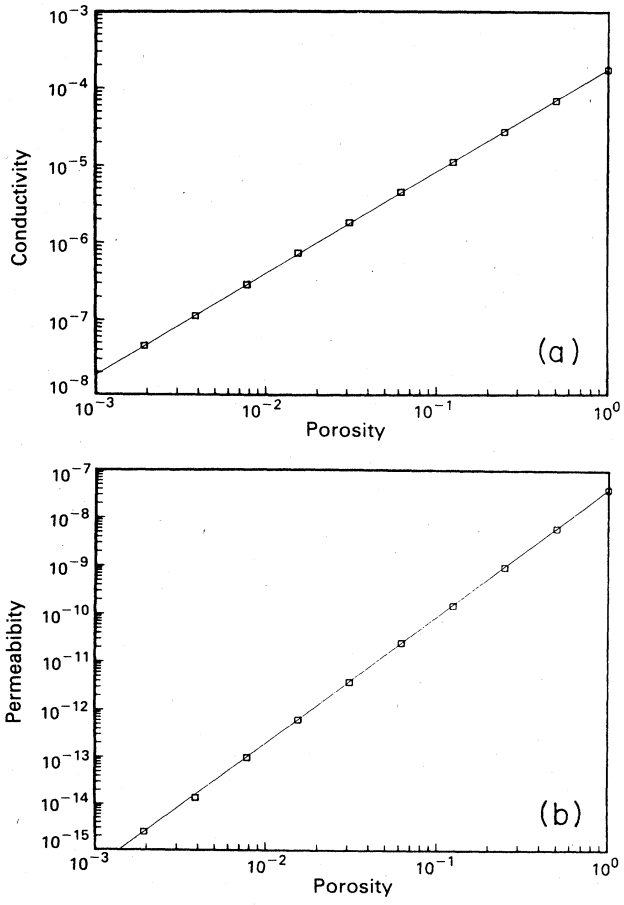


FIG. 2. Numerical results for the 2D $40\times41$ sample with shrinking factor $x=0.75$: (a) conductivity vs porosity ($m=1.32$), and (b) permeability vs porosity ($m'=2.68$).

set of typical results for a $40\times41$ sample with $x=0.75$. We can see that both $G_{nw}$ and $k_{nw}$ have a simple power-law dependence on $\phi$. In this particular case, we find $m=1.32$ and $m'=2.68$, which differ from the values predicted by the 1D calculation.

To confirm that this finding is not fortuitous, we perform the same calculation for $d=2,3,4,5$, using different sample sizes and $x$ values: $L$ ranges from 5 to 60, $x=0.25$, 0.50, and 0.75. Indeed, we find power laws in each case. The values of $m$ and $m'$ we obtained are tabulated in Table I. Several interesting observations can be made from these results.

(1) $m$ and $m'$ increase with decreasing $x$, as in the 1D case, but their values are always smaller than the 1D values given by Eqs. (10) and (11), which are listed in the first row of Table I.

(2) Except in the $x=0.25$ case where we were unable to obtain reliable values for $k_{nw}$ due to numerical problems, we find that $m'\approx 2m$ regardless of $d$ and $L$. This relationship is also different from that in 1D [Eq. (11)].

(3) Although $m$ and $m'$ seem to decrease with increasing $d$ in Table I, we note that they increase with $L$ for $d\geq 3$, which means that our results are affected by the finite-sample size in these higher dimensions. Taking that into consideration, the results suggest that $m$ and $m'$ are independent of $d$ for $d\geq 2$.

(4) In addition to using a flat initial distribution for the $r_i$'s, we have also tried other initial distributions in several cases and found no effect on $m$ and $m'$. From Eqs. (6) and (7), we can see that this is to be expected since the average over $P(n)$ is decoupled from the average over the initial distribution.

### C. Analytical estimates in higher dimensions

Some insights into the above results can be obtained by analyzing the model in the thermodynamic limit, i.e., when $M,N$ and $M/N\rightarrow\infty$. By the central-limit theorem, we know that the shrinkage probability $P(n)$ in Eq. (4) becomes a Gaussian distribution centered at $\bar{n}=M/N$ with a width $\delta n=(\bar{n})^{1/2}$. $\bar{n}$ is the most probable value of $n$ as well as its average. By our construction, however, the *most probable* value of a conductance $G_i^{mp}$ is

$$G_i^{mp}=x^{2\bar{n}}G_i\ , \tag{12}$$

which is *not* the same as the *average* value $\bar{G}_i$ in Eq. (5). The reason is that the amount of change in $G_i$ at any particular shrinking step is dependent on the value of $G_i$ at that time and the central-limit theorem *does not* apply under such conditions. (Similar behavior should also occur in real rocks, since we expect the smaller channels in the rocks to have smaller changes in their cross sections regardless of what the reduction process is.) In the limit that $\bar{n}\rightarrow\infty$, fluctuations of order $(\bar{n})^{1/2}$ are unimportant and we can assume $G_i^{mp}$ appears in Kirchoff's equations. We expect, therefore, the network conductance $G_{nw}$ to be

$$G_{nw}\propto G_i^{mp}\propto x^{2M/N}\ . \tag{13}$$

Combining this with Eq. (5), we have

$$m=\lim_{N,M,M/N\rightarrow\infty}\frac{\ln x^{2M/N}}{\ln[1+(x^2-1)/N]^M}=\frac{\ln x^2}{x^2-1}\ . \tag{14}$$

For the permeability exponent $m'$, we note that since $k_i\propto r_i^4\propto G_i^2$, it follows immediately from the above equation that

$$k_{nw}\propto x^{4M/N}\ \text{and hence}\ \ m'=2m\ . \tag{15}$$

The values of $m$ and $m'$ calculated from these equations are given in the last row of Table I. They are in good agreement with the numerical results, especially with those in two (2D), dimensions where we have been able to study larger sample dimensions. The agreement worsens with increasing $d$ and decreasing $x$. The former can be attributed to the limitation in our sample size as mentioned above. The latter is probably due to the fact that when we reduce $\phi$ by the same amount, $M/N$ is smaller for a smaller value of $x$. The crucial step in deriving Eqs. (14) and (15) is that we assumed $G_{nw}\propto G_i^{mp}$. This approximation can have an error of the order of $x^{2\delta n}$, which will lead to a correction in Eq. (14) of the order of $\delta n/\bar{n}=(M/N)^{-1/2}$. One expects, therefore, a worse

TABLE I. Numerical values for $m$ and $m'$ obtained from simple cubic networks of different sizes $L$ in different dimensions $d$. Three values for the shrinking factor $x$ were tried. The top row gives the 1D exact values. The bottom row gives the analytical values in higher dimensions.

| | $x=0.25$ | | $x=0.5$ | | $x=0.75$ | |
|---|---|---|---|---|---|---|
| | $m$ | $m'$ | $m$ | $m'$ | $m$ | $m'$ |
| 1D | 16.00 | 272.00 | 4.00 | 21.00 | 1.78 | 4.94 |
| $10^2$ | 2.80 | | 1.85 | 3.73 | 1.32 | 2.67 |
| $20^2$ | 2.83 | 5.35 | 1.85 | 3.70 | 1.33 | 2.67 |
| $40^2$ | 2.91 | | 1.83 | 3.73 | 1.32 | 2.68 |
| $60^2$ | 2.86 | | 1.86 | 3.75 | 1.33 | 2.70 |
| $5^3$ | 2.31 | 4.20 | 1.57 | | 1.23 | 2.48 |
| $10^3$ | 2.49 | 4.73 | 1.68 | 3.32 | 1.26 | 2.48 |
| $15^3$ | 2.55 | | 1.73 | 3.29 | 1.25 | 2.50 |
| $5^4$ | 2.33 | 4.52 | 1.55 | 3.04 | 1.20 | 2.39 |
| $8^4$ | 2.37 | | 1.58 | 3.08 | 1.23 | 2.41 |
| $5^5$ | 2.22 | 4.17 | 1.53 | 2.96 | 1.19 | 2.33 |
| $\frac{\ln(x^2)}{x^2-1}$ | 2.96 | 5.95 | 1.85 | 3.70 | 1.32 | 2.63 |

agreement with the numerical results for a smaller $x$. In practice, however, we find that the disagreement is much less than $(M/N)^{-1/2}$.

A more rigorous argument for Eq. (13) may be given in terms of upper and lower bounds on the network conductivity.[12-14] Suppose for simplicity's sake that we let all the initial bonds have a conductance of unity. In the thermodynamic limit, they will fall in the range

$$G_l \equiv x^{2(\bar{n}-\delta n)} < G_i < x^{2(\bar{n}+\delta n)} \equiv G_u$$

with an exponentially small number of exceptions. A lower bound on the network conductance is obtained by replacing all $G_i < G_l$ with 0 and all $G_i \geq G_l$ with $G_l$, and thus $G_{\rm nw} > bG_l$. The constant $b$ is a function of the network geometry, and corresponds to the conductance of a network where most bonds have unity conductance and an exponentially small fraction have zero conductance, and $b$ is therefore a finite number. Similarly, an upper bound of the network conductance follows by replacing all $G_i > G_u$ by infinity and all others by $G_u$, and we have $G_{\rm nw} < b'G_u$. In the limit $\bar{n} \to \infty$, fluctuations of order $\delta n$ are negligible and the two bounds converge to the *most probable* value, and we obtain Eq. (13).

We expect Eqs. (14) and (15) to be correct for an infinite system in the large-$M/N$ limit, i.e., when $\phi \to 0$. They explain all the findings from the numerical calculations. In addition, these analytical results allow us to see explicitly that *$m$ is related to the difference between the most probable conductance $G_i^{\rm mp}$ and the average conductance $\bar{G}_i$. The parameter $x$ is simply a measure of that difference or, in other words, the skewness of the distribution. The smaller $x$ is, the more skewed is the distribution, and the larger is $m$.* Applying this knowledge to rocks, we can qualitatively explain the difference of $m$ values for the two sandstones in Fig. 1. For the Cotton Valley sandstone, we see that it has a small number of larger pores which are connected via a large number of much smaller pores. This implies that the pore-size distribution for this rock is more skewed than the Berea sandstone and hence its $m$ value should be larger, which is what we observed. In the next section, we will demonstrate this behavior in synthetic rocks in a more systematic way.

Another interesting prediction of the model is that for any $d \geq 2$, the properties of the network are simply related to the statistical distribution of the individual elements, regardless of how they are connected in detail. This leads to Eq. (15), which relates the conductivity and permeability in a very simple way. It is common to use the *formation factor* ($F \equiv \sigma_w/\sigma_r = a\phi^{-m}$) to describe the conductivity of rocks, and Eq. (15) suggests that the permeability may follow the law

$$k_r \propto F^{-2} . \tag{16}$$

[Note that this relationship would be rigorous if $a$ in Eq. (1) were a universal constant, which is not established.] In the next section, we will show permeability data to support this prediction.

## III. EXPERIMENTS

To test some of the findings of the model, we performed conductivity and permeability experiments on artificial rocks made of fused glass beads. The glass beads were obtained from the Ferro Corporation and sifted into three size groups: 44–53 $\mu$m, 88–105 $\mu$m, and 177–210 $\mu$m. They were washed first in dilute hydrochloric acid and then in water. Low-density particles were removed by water flow and magnetic particles were removed by a 6-kOe field. Several melts with different porosities were made from each of the size groups by fusing them to different degrees. Cylindrical samples 1.5 in. long and 0.75 in. in diameter were cut from each melt. To saturate the samples with salt water, they were first placed in a vacuum to remove the air in the pore space and the water was then let into the evacuated container to fill the pores. The porosity of each sample was determined by measuring its dry weight, wet weight, and buoyancy in water. These measurements also give the grain density $\rho_g$ of the sample. For samples with $\phi \gtrsim 0.03$, we find $\rho_g$ in the range $2.485 \pm 0.010$ gm/cm$^3$, in agreement with the value for bulk glass. From the small spread in the measured grain density, we can infer that there were essentially no occluded volumes in these samples (less than 1% volume fraction if they exist), i.e., the pore space is completely connected and can be fully saturated by the water. In addition, we can also estimate that the accuracy of the porosity measurement is about 0.01. In samples with $\phi \lesssim 0.03$, we find some samples with significantly lower values of $\rho_g$, implying the existence of occluded volumes at such low porosities. We did not study those samples further.

To make conductivity and permeability measurements, the samples were fitted inside a Hassler collar which is a double-wall cylinder with a length and inner diameter matching those of the sample. The inner wall of this device is made of neoprene and the outer wall is made of steel. Air can be injected between the two walls to pressurize the neoprene sleeve inward to grasp the sample tightly. This prevents fluid or current leakage along the wall. Four-terminal ac conductivity measurements were made by using an impedance meter. The electrodes were made of silver and chlorodized. The voltage electrodes were placed against the ends of the Hassler collar and the sample, and the current electrodes were far away from them. To ensure that the measurements were not affected by electrode-polarization effects, we varied the measurement frequency (100 Hz, 1 kHz, and 10 kHz) and voltage (50 mV and 1 V), and no significant effects were observed. In permeability measurements the sample was placed vertically with water injected at the bottom and extracted at the top. When the permeability of the sample is high [$k_r \gtrsim 100$ md (millidarcy)], the pressure gradient across the sample was determined by the difference in water level between the inlet and outlet reservoirs. When the permeability is low ($k_r \lesssim 100$ md), higher pressures were obtained by using a piston with a regulator. The flow rate was determined by measuring the amount of water collected at the outlet and the time it took to collect it. The former varied between 0.1 and 50 cm$^3$, the latter varied between 1

and 50 min. The results of these experiments are described below.

### A. Conductivity and formation factor

The main interest in conductivity measurements is to determine the *formation factor* $F$ as a function of porosity, to test Archie's law. We typically measure the sample conductivity $\sigma_r$ for three or four different water conductivities ($\sigma_w$) which varied between 0.24 and 7.7 $\Omega^{-1}\,m^{-1}$. A linear least-square fit of $\sigma_r$ versus $\sigma_w$ gives a slope equal to $F^{-1}$ for that sample. A total of 26 samples were measured and the results are summarized in Fig. 3, where we plotted $F$ versus $\phi$ on a log-log scale. The porosity ($\phi$) ranges from 0.023 to 0.399. The dashed line in Fig. 3 represents the theoretical prediction of the spherical grain self-similar model, which has $a=1$ and $m=3/2$.[7-10] In Ref. 7, data down to $\phi\approx 0.026$ were shown and they agreed with this prediction. A subsequent study of Johnson *et al.*,[15] however, disagreed with those results with data down to $\phi\approx 0.10$. Our data in Fig. 3 agree with the latter results, extending the porosity range down to $\phi=0.023$ and varying the grain size of the sample. We observe that the data in the porosity range $0.2\lesssim\phi\lesssim 0.4$ can be approximated by the self-similar model prediction. For $\phi\lesssim 0.2$, however, the value of $F$ is always higher than the prediction, implying a higher value for $m$.

There are two possible ways to characterize the low-porosity data. First, it can be approximated by the solid line in Fig. 3, which corresponds to $a\approx 3.3$ and $m\approx 2.3$, i.e., both $a$ and $m$ are constants over a large porosity range. Alternatively, if we assume $a=1$, we can define $m=d(\ln\sigma)/d(\ln\phi)$ and say that $m$ increases continuously with decreasing porosity. The high-porosity data points correspond to $m\approx 1.5$ and the low-porosity data points correspond to $m\approx 2$. Either way, $m$ is higher for lower porosity. Such a trend can be qualitatively understood by studying the microgeometry of the samples. In Fig. 4, we show the micrographs of two samples with different porosities. We can see that the high-porosity one ($\phi=0.315$) has a more uniform pore-space distribution, much like the Berea sandstone in Fig. 1. In contrast, the low-porosity sample ($\phi=0.061$) shows a larger fluctuation in its pore-space distribution. Similar to the Cotton Valley sandstone in Fig. 1, it has a small number of large isolated pores

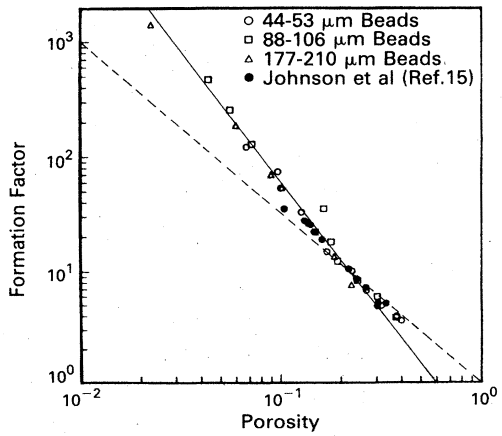


FIG. 3. Formation factor for different fused-glass-beads samples as obtained by resistivity measurements. The dashed line is the prediction of the self-similar model for spherical grains ($a=1$, $m=\frac{3}{2}$). Data below 20% porosity show substantial deviation from the prediction. They can be approximated by the solid line, which corresponds to $a=3.3$ and $m=2.3$.

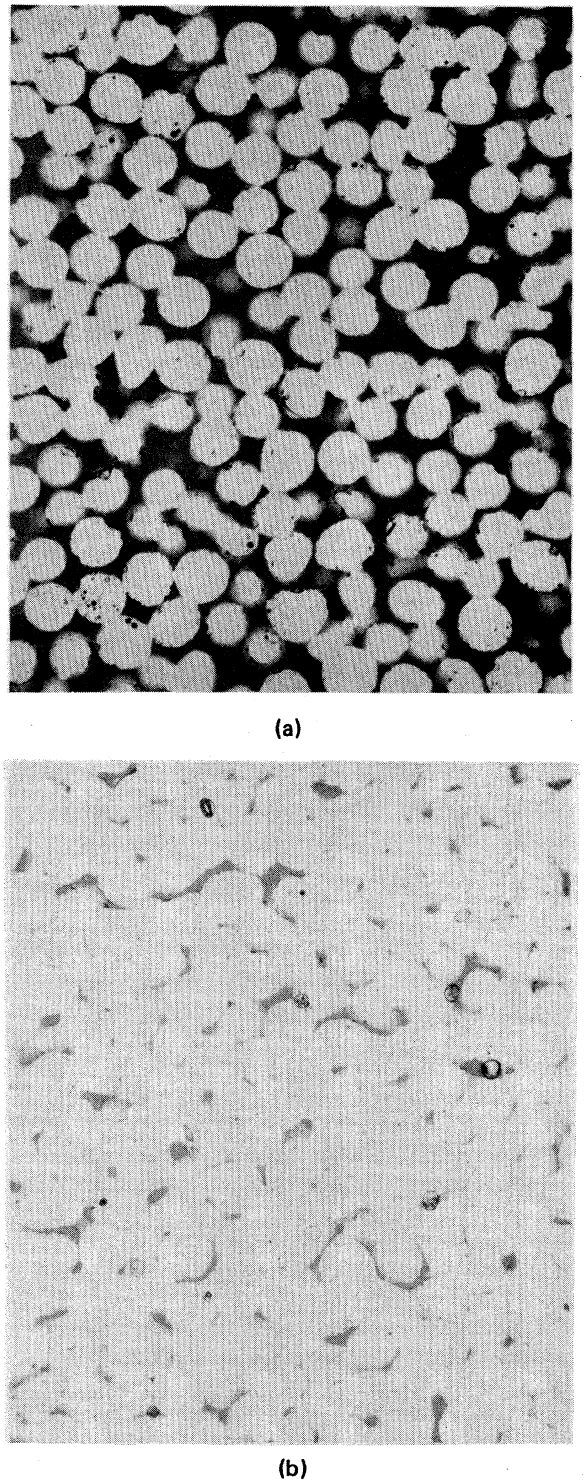


FIG. 4. Micrographs of two fused-glass-beads samples with different porosities: (a) $\phi=0.315$, and (b) $\phi=0.061$. Their contrasting microgeometry is similar to the two sandstones in Fig. 1.

connected via much smaller pores. Following the discussion in the preceding section, one expects the latter samples to have higher $m$ values, which is exactly what we found. Furthermore, since the pore-space distribution changes continuously with $\phi$, it is perhaps more reasonable to think of $m$ as also continuously varying with $\phi$, rather than being constant over a wide range of $\phi$. The permeability results described below will further support this view.

### B. Permeability

Since fluid-flow experiments can be performed on the same sample that electrical measurements are made, one can readily test how the permeability is related to the conductivity or the *formation factor,* i.e., one can test Eq. (16). To determine the permeability, we measured the flow rate at three or four different pressure gradients across the sample. A linear least-square fit of the two quantities gives a slope equal to $k_r/\mu$, where $\mu$ is the viscosity of water. Unlike the *formation factor* which is dimensionless and independent of the grain size, $k$ has the dimension of (length)$^2$ and hence must depend on the grain size. In Fig. 5 we show a log-log plot of $k_r$ versus $F$. We can see that the data points fall into three groups corresponding to the three different grain sizes we used. Within each group, the data can be approximated by a straight line with a slope of $-2$, in agreement with Eq. (16). Some data points deviate from the straight lines when the permeability is below 10 md. They may be due to the fact that some channels become completely blocked in the low-porosity samples since we know that there are occluded volumes when the porosity is below 3%. Another possible explanation will be given in the next section. We should mention, however, that there are difficulties in measuring a small permeability. Because the flow rate is low, high-pressure gradients across the sample and high pressure in the Hassler collar must be maintained over a long period of time. As a result, there can be small fluid or air leakages in the measuring system which can lead to large errors in the results.

We note that the network model only predicts

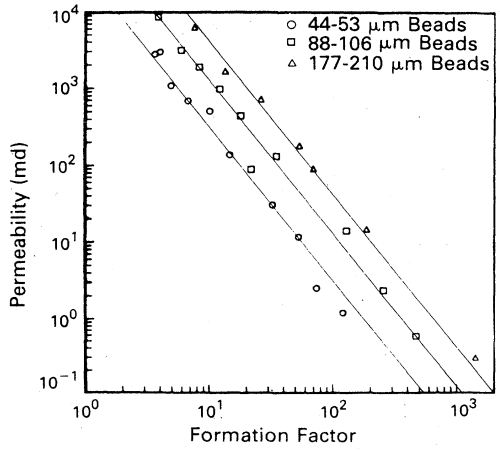


FIG. 5. Log-log plot of permeability vs formation factors for fused-glass-beads samples with different grain sizes. For each grain size, the relationship $k_r \propto F^{-2}$ is approximately obeyed.

$k_{nw} \propto \phi^{2m}$. If $a$ has different values for high and low porosities, one would not expect Eq. (16) to hold for all porosities. Since the data in Fig. 5 actually cover both $\phi > 0.2$ and $\phi < 0.2$, it *suggests* that one may indeed have $a = 1$ at all porosities and consider $m$ as the single parameter that characterizes the pore-size distribution, which varies continuously with $\phi$. In a large rock formation, it is conceivable that the local porosity varies over a wide range and the distribution is similar throughout, in which case Archie's law with a single value of $m$ can apply.

## IV. DISCUSSION

The main conclusion that we can draw from our results is that *the scaling behavior of both the conductivity and the permeability of rocks are determined by the skewness of their pore-size distribution.* The skewness results from the rock-formation process which tends to reduce the large pores by a large amount and the small pores by a small amount. Such a process will generally produce a pore-size distribution which is *log-normal,* instead of *normal.* There is, in fact, ample empirical evidence that both the pore- and grain-size distributions in rocks are roughly described by a log-normal distribution.[16,17] Our model, in essence, shows how this microgeometrical property can be related to the macroscopic properties such as the conductivity and permeability.

We use the term pore-space (-size) distribution loosely since there is no mathematically precise definition for it. [5] It has a well-defined meaning only in simple models, such as ours, which approximate the pore space as a network of tubes. Such an approximation may be justified when one is dealing with physical properties that are associated with a length scale that is larger than the characteristic grain size (of order 100 $\mu$m), and conductivity and permeability are among such properties. On the submicron length scale, there is some evidence that the pore space of a rock may have fractal characters,[18] in which case it will not be appropriate to think in terms of *most probable value, average value,* etc. *On the length scale of the grain size, however, it is reasonable to represent the space between two grains as a tube with a length comparable to the grain size and a cross-section that varies along the length, like our 1D network. On a still larger scale, one can assign a uniform effective radius to each tube and envision them being connected at "nodes" to form a network, like a higher-dimension network.* Although we neglected the nodes in our model, it is easy to see what they will do. *The nodes are basically pocketlike; they contribute much to the porosity and little to the conductivity and permeability.* In other words, they add to the skewness of the pore-space distribution and increase the value of $m$. Since our model is not intended to predict an absolute value of $m$, neglecting the nodes is permissible. Likewise, the artificial process of shrinking the tubes continuously by a constant factor $x$ is only a way to generate a simple distribution that makes the network analytically tractable. Had we used a distribution of $x$ values, the conductance distribution will be more complicated but the scaling-law solution of the model in the $\phi \rightarrow 0$ limit should be unchanged. In 1D for example, Eqs. (5)—(10) can be followed through with any

skewed distribution which gives different values for $\overline{G_i}$ and $\overline{G_i}^{-1}$. In higher dimensions as long as the conductance distribution is broad (like a log-normal distribution), the heuristic arguments given in Sec. II should apply regardless of how the distribution is obtained in detail. Conversely, we note that the agreement between the numerical results and Eq. (14) demonstrates the validity of those arguments in the $\phi \to 0$ limit.

The advantage of the analytic arguments is that they allow us to make a simple correlation between the permeability and the conductivity exponents: $m'=2m$, and the data on fused glass beads provide good support for this prediction. It is interesting to note that the simple power-law expression in Eq. (11) for the permeability can be rewritten in the form of the Kozeny equation. The surface-to-volume ratio $S_0$ in our model is proportional to the average tube radius $\langle r_i \rangle$. Following Eqs. (5) and (8), we have

$$S_0 \propto \langle x \rangle \propto \left[1+\frac{x-1}{N}\right]^M \propto \phi^q ,$$

where

$$q = \lim_{N\to\infty} \frac{\ln\left[1+\frac{x-1}{N}\right]^M}{\ln\left[\frac{1+x^2-1}{N}\right]^M} = \frac{1}{1+x} < 1 .$$

Substituting this result into Eq. (11) gives

$$k_r \propto \frac{\phi^{m''}}{S_0^2} \quad \text{where } m''=m'+2q . \tag{17}$$

Except for the fact that $m''$ is variable, this expression is identical to the Kozeny equation. It should be emphasized, however, that there is considerable data on other materials which do not fit the Kozeny equation and many modified forms have been proposed.[6] In particular, simple power laws like Eq. (11) with various exponents $m'>3$ and without the $1/S_0^2$ factor have been suggested by different studies. The variation in $m'$ in these studies is consistent with the point of view taken here, since we predict the permeability exponent $m'$ to be nonuniversal just like the conductivity exponent $m$, and the latter is empirically well known to be nonuniversal. The data presented here are not sufficient to distinguish whether Eq. (11) or Eq. (17) is more preferable. It will be interesting to perform a more extensive study that includes measurements of $S_0$ to test these relationships further.

Finally, it is important to make clear that the higher-dimension result $m'=2m$ in our model is a consequence of assigning a uniform radii to the tubes. In any real sample, the cross-sectional area of a conduction channel varies along its length. Provided that this variation is not too severe (i.e., it does not have a broad log-normal–like distribution), the uniform radii approximation should be valid. Otherwise, one would expect the one-dimensional behavior [Eqs. (10) and (11)] to play an important role. In the latter case, since the 1D analysis gives $m'=m(m+1)>2m$, one expects

$$2m \le m' \le m(m+1) . \tag{18}$$

We note that in Fig. 5, the deviations of the low-porosity data points, although can be explained otherwise, are consistent with $m'>2m$.

## ACKNOWLEDGMENTS

We are grateful to B. I. Halperin and A. B. Harris for helping us to understand the numerical results, J. Banavar, D. L. Johnson, W. Murphy, and D. J. Wilkinson for helpful discussions, and L. P. Kadanoff for encouraging this work. Special thanks are due to our colleagues in the Rock Laboratory at the Schlumberger-Doll Research Center who provided extensive assistance in sample preparation and some of the measurements.

[1]G. E. Archie, AIME Trans. **146**, 54 (1942).
[2]G. V. Keller, in *Handbook of Physical Properties of Rocks*, edited by R. S. Carmichael (CRC, Boca Raton, Florida, 1982).
[3]J. Kozeny, Sitzungsber. Akad. Wiss. Wien **136**, 271 (1927).
[4]P. C. Carman, *Flow of Gases Through Porous Media* (Academic, New York, 1956).
[5]A. E. Scheidegger, *The Physics of Flow in Porous Media* (University of Toronto Press, Toronto, 1974).
[6]F. A. L. Dullien, *Porous Media, Fluid Transport and Pore Structure* (Academic, New York, 1979).
[7]P. N. Sen, C. Scala, and M. H. Cohen, Geophysics **46**, 781 (1981).
[8]D. A. G. Bruggeman, Ann. Phys. (Leipzig) **24**, 636 (1935).
[9]P. N. Sen, Geophysics **46**, 1714 (1981); see also K. Mendelson and M. H. Cohen, *ibid.* **47**, 257 (1982); P. N. Sen, *ibid.* **49**, 586 (1984).
[10]R. E. De la Rue and C. W. Tobias, J. Electrochem. Soc. **106**, 827 (1959).
[11]G. W. Milton, in *Physics and Chemsitry of Porous Media (Schlumberger-Doll Research)*, edited by D. L. Johnson and P. N. Sen (AIP, New York, 1984), p. 66.
[12]V. Ambegaokar, B. I. Halperin, and J. S. Langer, Phys. Rev. B **4**, 2612 (1971).
[13]V. K. S. Shante, Phys. Rev. B **16**, 2597 (1977).
[14]S. Kirkpatrick, in Proceedings of the Seminar on Electrons in Disordered Systems, Kyoto, 1972 (unpublished).
[15]D. L. Johnson, T. J. Plona, C. Scala, F. Pasierb, and H. Kojima, Phys. Rev. Lett. **49**, 1840 (1982).
[16]E. Pittman, in *Physics and Chemistry of Porous Media (Schlumberger-Doll Research)*, edited by D. L. Johnson and P. N. Sen (AIP, New York, 1984), p. 1.
[17]G. S. Visher, J. Sediment. Petrol. **39**, 1074 (1969).
[18]D. Avnir, D. Farin, and P. Pfeifer, Nature **308**, 261 (1984).

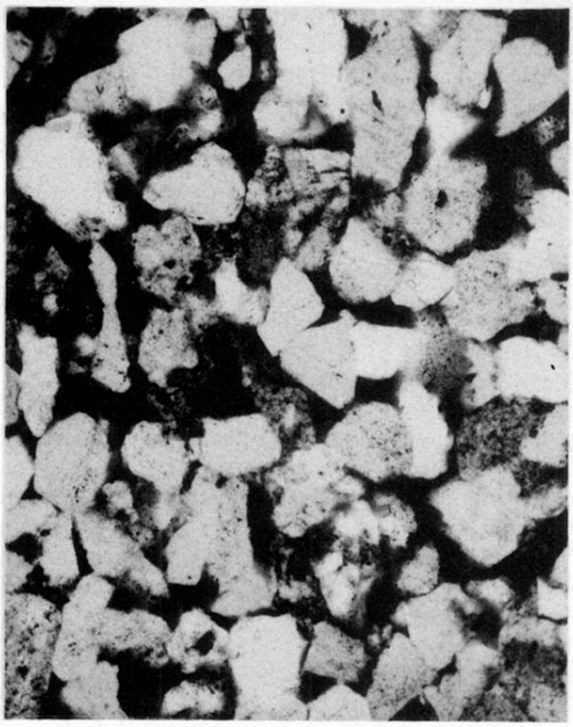

(a)

(b)

(c)

FIG. 1. Thin section micrographs of (a) Berea sandstone (100×), (b) Cotton Valley sandstone (100×) and (c) Indiana limestone (25×). The pore space in (a) and (b) are dark whereas, in (c), it is bright. The grain shapes of (a) and (b) are very similar, but they have different $m$'s. The grain shapes of (b) and (c) are very different, but their $m$ values are essentially the same.

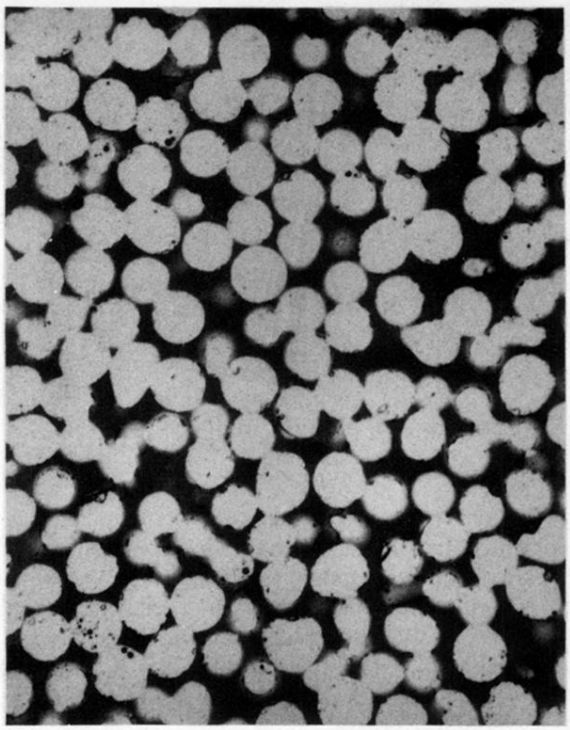

(a)

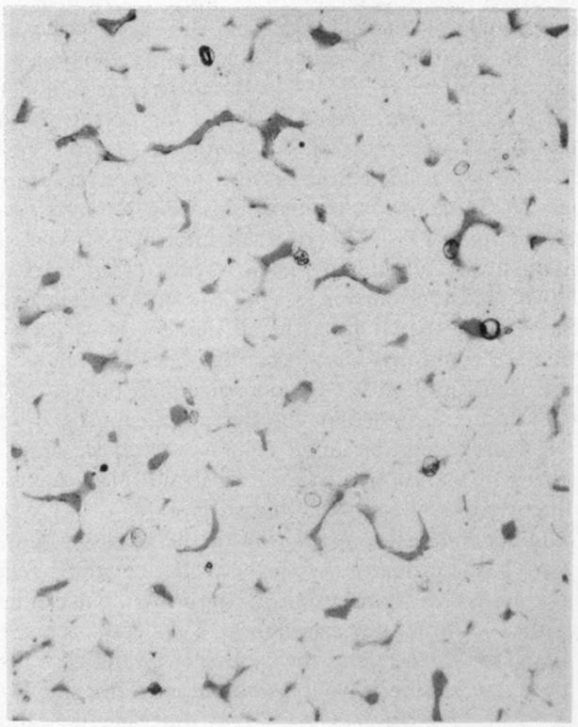

(b)

FIG. 4. Micrographs of two fused-glass-beads samples with different porosities: (a) $\phi = 0.315$, and (b) $\phi = 0.061$. Their contrasting microgeometry is similar to the two sandstones in Fig. 1.